Theoretical Studies on Cycloaddition Reactions between 1-Aza-2-azoniaallene Cations and Isocyanates

Mei-Ju Wei,[a] De-Cai Fang,*[a] and Ruo-Zhuang Liu[a]

Keywords: 1-Aza-2-azoniaallene cations / [3+2] Cycloaddition / Isocyanates / Reaction mechanisms

The mechanisms of the title reactions between 1-aza-2-azoniaallene cations and isocyanic acid or isocyanates have been theoretically explored at the B3LYP/6-31++G** level. It was found that all of these reactions proceed in asynchronous but concerted pathways. The substituent effects are also obvious; e.g., the presence either of an electron-withdrawing chlorine substituent on the 1-aza-2-azoniaallene cation or of an electron-releasing methyl substituent on the isocyanate both favor the cycloaddition reactions. For the [1,2]-shift reactions, all the substituents lower their activation barrier, especially Cl substituents on the 1-aza-2-azoniaallene cation, but when Cl substituents are present on the 1-aza-2-azoniaallene cation the rearrangement product is not as stable as others. In addition, solvent effects with the PCM model are also reported, and a model reaction has been investigated at the MP2/6-31+G* and QCISD/6-31+G* levels as well as by DFT. (© Wiley-VCH Verlag GmbH & Co. KGaA, 69451 Weinheim, Germany, 2004)

Introduction

1,3-Dipolar cycloaddition reactions of neutral 1,3-dipoles have developed into a generally practical method for five-membered heterocyclic-ring synthesis,[1] and these reactions have been extensively studied both experimentally[2] and theoretically.[3] Recently, cycloadditions of cationic four-electron, three-center components with multiple bonds, which open up a new and potentially useful route for the construction of five-membered heterocycles, have aroused chemists' interest.[4] The novel cationic four-electron, three-center components, 1-aza-2-azoniaallene cations, are generated as reactive intermediates in many oxidative processes of hydrazones[5] or are obtained from 1-chloroalkyl azo compounds by treatment with Lewis acids such as $SbCl_5$ or $AlCl_3$ [6a] at low temperatures. The cations are reactive and can undergo cycloadditions with multiple bonds through [3+2] cycloaddition reactions.[6] This subject is one of our research projects, dedicated to study the mechanisms of cumulene cations.[7]

In 1994, Jochims and co-workers found that the strongly electrophilic 1-aza-2-azoniaallene salts react with isocyanates to furnish 4,5-dihydro-5-oxo-3*H*-1,2,4-triazolium salts or 4,5-dihydro-5-oxo-1*H*-1,2,4-triazolium salts after isomerization.[6d,6i] In addition, the 4,5-dihydro-5-oxo-3*H*-1,2,4-triazolium salts can be prepared by treatment of geminal azoalkyl isocyanates with acids[8a,8b] or by alkylation of 5,5-disubstituted 4,5-dihydro-3*H*-1,2,4-triazol-3-ones.[8c] Many experiments have shown that 1,2-rearrangement in 1,2,4-triazolium salts can take place spontaneously, on heating or on treatment with acids.[6i,6d,9a−9d] The primary ab initio works for the rearrangements were performed by Kroemer and co-workers,[9e,9f] who predicted that a [1,2]-shift from a carbon atom to an electron-deficient nitrogen atom would not be a nucleophilic rearrangement, and migratory aptitudes are predicted to be in the order isopropyl > ethyl > methyl on the basis of HF/6-31G* and MP2/6-31G*//HF/6-31G* calculations. Wang et al.[6i] have carried out some semiempirical AM1 calculations to explain the mechanism together with their experiments. However, to the best of our knowledge, a high-level calculation has not yet been done for the title reactions. In this paper, the mechanism and solvent and substituent effects of the title reaction have been investigated by theoretical calculations. The studied reactions are shown in Scheme 1.

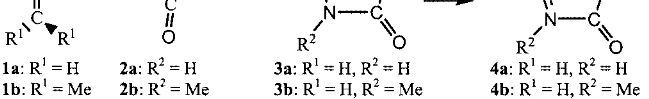

1a: $R^1 = H$
1b: $R^1 = Me$
1c: $R^1 = Cl$

2a: $R^2 = H$
2b: $R^2 = Me$
2c: $R^2 = Cl$

3a: $R^1 = H, R^2 = H$
3b: $R^1 = H, R^2 = Me$
3c: $R^1 = H, R^2 = Cl$
3d: $R^1 = Me, R^2 = H$
3e: $R^1 = Cl, R^2 = H$

4a: $R^1 = H, R^2 = H$
4b: $R^1 = H, R^2 = Me$
4c: $R^1 = H, R^2 = Cl$
4d: $R^1 = Me, R^2 = H$
4e: $R^1 = Cl, R^2 = H$

Scheme 1

---

[a] Department of Chemistry, Beijing Normal University,
100875 Beijing, People's Republic of China
Fax: (internat.) + 86-10-58805422
E-mail: dcfang@bnu.edu.cn

Supporting information for this article is available on the WWW under http://www.eurjoc.org or from the author.

DOI: 10.1002/ejoc.200400343

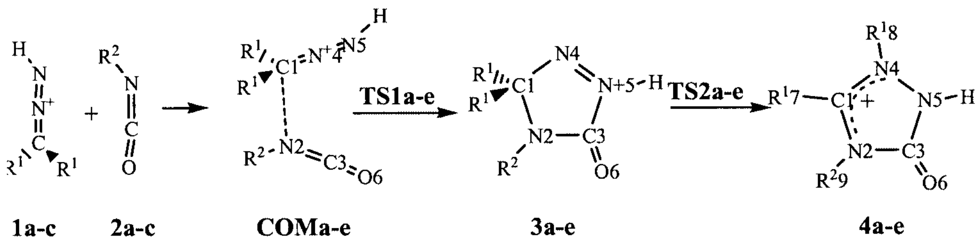

Scheme 2

Results and Discussion

The Model Reaction $H_2C=N^+=NH$ + HNCO

The reaction was first investigated in the gas phase. The geometries of the reactants (**1a** and **2a**), complex (**COMa**), transition states (**TS1a** and **TS2a**), and products (**3a** and **4a**) were optimized at the B3LYP/6-31++G**, MP2/6-31+G*, and QCISD/6-31+G* levels, respectively, and all the stationary points were characterized by vibrational frequencies at the corresponding levels. The atomic numbering systems of these stationary points are shown in Scheme 2 (more detailed information is given in Figure S1 of the Supporting Information; see also footnote on the first page of this article), and the optimized parameters, frequencies, and energies are also listed in Tables S1−S3 of the Supporting Information, respectively.

B3LYP/6-31++G** predicts the 1-aza-2-azoniaallene cation (**1a**) to be an approximately linear molecule with the hydrogen atom connected to the nitrogen atom almost on the same plane as its skeleton atoms, while the plane of the methylene group is perpendicular to the C−N−N plane.[7a] From the structural parameters, it can be seen that the other reactant, isocyanic acid (**2a**), is also a planar molecule, and the atoms N, C, and O are nearly linear, with the bond angle being 172.2°.

When reactant **2a** approaches **1a**, a complex **COMa** is formed, owing to the favorable electrostatic interaction of the reactants (the charges of NH group and CH_2 group are −0.25 and +0.28e, respectively), with the N2−C1 bond length at the B3LYP/6-31++G** level being 2.734 Å. When the two reactants approach more closely, the product 4,5-dihydro-5-oxo-3*H*-1,2,4-triazolium ion (**3a**) is formed via a transition state **TS1a**, in which the N5−N4−C1 angle becomes 140.0° from the original 167.1°, and the N2−C1 and N5−C3 distances are 2.092 and 3.371 Å, respectively. It is therefore an asynchronous but concerted [3+2] cycloaddition reaction. However, the N4−C1 distance in **TS1a** is 1.307 Å, 0.052 Å longer than that in **3a**. From the reactants to **TS1a**, the C3−O6 distance does not greatly change (1.175, 1.165, and 1.156 Å in **2a**, **COMa**, and **TS1a**, respectively). In addition, the N4C1N2C3 and H9N2C1N4 torsion angles in **TS1a** are −36.6 and 144.8°, which could be elucidated in terms of frontier orbital interactions (see Figure 1). From Figure 1 it can be seen that two types of orbital interactions are involved in the bonding process: the interaction between the LUMO+1 of **1a** and the HOMO of **2a** and the interaction between the LUMO+1 of **1a** and the HOMO−1 of **2a**. Because of the mismatching of orbital interaction or lower energy of the HOMO of **1a**, the LUMO and HOMO of **1a** seem not to be involved in the reaction. Product **3a** is a five-membered heterocycle with the C1−N2, N2−C3, C3−N5, N5−N4, and N4−N1 bond lengths being 1.438, 1.353, 1.547, 1.237, and 1.455 Å, respectively, the C3−N5 bond length thus being about 0.1 Å longer than a normal single C−N bond. All the atoms except for the two hydrogen atoms connected to the methylene group are in the same plane, and the bond lengths are in good agreement with structural measurement of 1,2,4-triazole derived from X-ray data.[8a] Product **3a** can undergo a hydrogen-shift (H-shift) reaction to produce **4a**, in which the main ring frame suffers from some distortion (e.g., N4−C1−N2−C3 = −0.4°; N5−N4−C1−N2 = −3.9°; and O6−C3−N2−C1 = −176.3°). During the H-shift process, the N2−C1, N4−C1, and N5−C3 bond lengths are all shortened by about 0.1 Å (N2−C1 = 1.331; N4−C1 = 1.318; N5−C3 = 1.401 Å in **4a**). On the other hand, the N5−N4 and C3−N2 bond lengths in **4a** are 0.143 and 0.087 Å longer than their counterparts in **3a**. The C1−N2 and C1−N4 bond lengths are shorter than a general C−N single bond, which shows that those bonds have some double bond characteristics. The transformation from

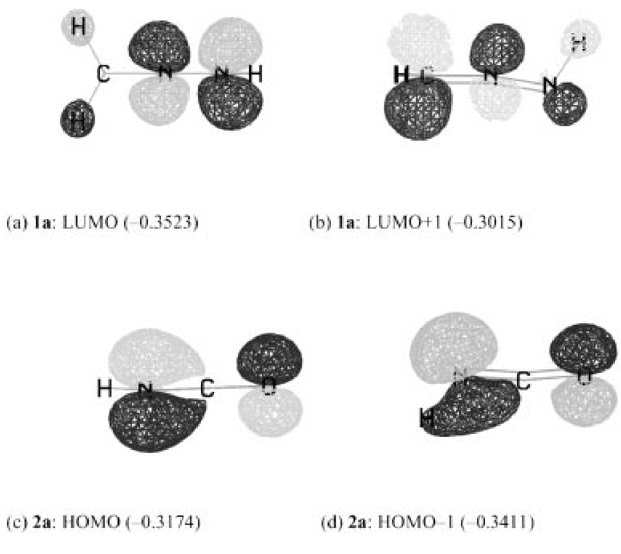

(a) **1a**: LUMO (−0.3523) (b) **1a**: LUMO+1 (−0.3015)

(c) **2a**: HOMO (−0.3174) (d) **2a**: HOMO−1 (−0.3411)

Figure 1. Sketch graphs and energies of the LUMO and LUMO+1 in **1a** and the HOMO and HOMO−1 in **2a**

3a to **4a** needs to pass through **TS2a**, in which the H8−C1 and H8−N4 distances are 1.322 and 1.369 Å, respectively.

The mechanism of the model reaction was also explored by MP2/6-31+G* and QCISD/6-31+G* methods. All stationary points were fully optimized and confirmed by the number of imaginary vibrational frequencies. It can be concluded from the geometry parameters (see Table S1 of the Supporting Information) that the structures of all the stationary points are similar to those at the B3LYP/6-31++G** level. The largest difference in bond length is 0.048 Å for the N2 and C1 distance in **TS1a**, and the maximum difference in bond angle is about 6.0° for the N4−C1−N2 angle in **COMa**.

The schematic potential energy surface for the model reaction (with zero-point energy correction) is given in Figure 2, from which it can be inferred that all the stationary points are below the reactant asymptote. **COMa** is 5.7 kcal/mol more stable than the reactants, because of favorable molecular interaction, and the energy of **TS1a** is 3.6 kcal/mol above **COMa**, but 2.1 kcal/mol below the reactants **1a** + **2a**. It is therefore obvious that the reaction **1a** + **2a** is quite facile, which is consistent with experimental findings,[6i] described by Wang et al. in 1994, that cycloaddition of 1-aza-2-azoniaalene salts to isocyanates occurred at −60 °C. Intermediate product **3a** might undergo a [1,2]-H-shift reaction via **TS2a**, with an activation barrier of 22.1 kcal/mol, to form the more stable **4a**, with an energy 26.1 kcal/mol lower than that of **3a**. IRC calculations, starting both from **TS1a** and from **TS2a**, confirmed that these transition states could reach the corresponding minima on both sides shown in Figure 2, which indicates that the obtained transition states are on the right reaction pathways.

The potential energy surfaces calculated at the MP2/6-31+G* and QCISD/6-31+G* levels are also shown in Figure 2, from which it can be seen that they are quite similar for different calculations. All the stationary point relative energies at the MP2/6-31+G* level are slightly lower than those at the B3LYP/6-31++G** level, but the activation barrier for rearrangement from **3a** to **4a** is 2.6 kcal/mol higher than that at B3LYP/6-31++G**. Similar trends are seen for QCISD/6-31+G* calculations.

In 1994, Wang et al. employed AM1 to study cycloadditions of MeNCO to Ar−N=N$^+$=C(Me)$_2$ or *t*Bu−N=N$^+$=C(Me)$_2$ [6i] and found a two-step reaction proceeding via acylium ion intermediates. Wang et al. also suggested, that it seemed premature to conclude that the cycloaddition reactions would generally occur in a non-concerted manner[6i] after considering errors inherent in the AM1 method and solvent effects. Although we were able to repeat the intermediate for the two-step process in the model reaction by the AM1 method, we failed to locate a similar intermediate at the B3LYP/6-31++G** level; thus, at the B3LYP/6-31++G** level the cycloaddition reaction is a concerted process. The same conclusions are obtained at the MP2/6-31+G* and QCISD/6-31+G* levels. The reaction mecha-

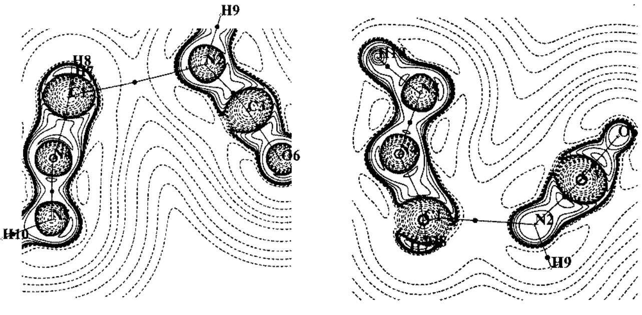

(a) **COMa** (b) **TS1a**

Figure 3. Molecular graphs and Laplacian distribution of some stationary points; in these figures, dashed lines denote positive values of $\nabla^2\rho_b$ and full lines stand for negative values of $\nabla^2\rho_b$; the bonded charge concentrations are indicated by solid squares; in addition, bond paths (heavy solid lines), bond critical points (solid circles) are shown for ρ(*r*)

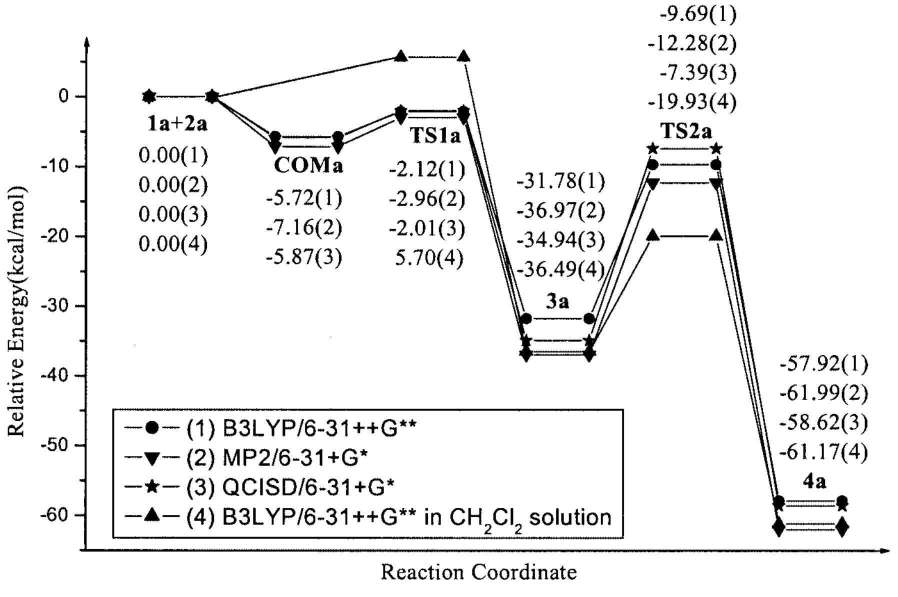

Figure 2. Schematic description of potential energy surfaces (with ZPE correction) for the model reaction (**1a** + **2a**)

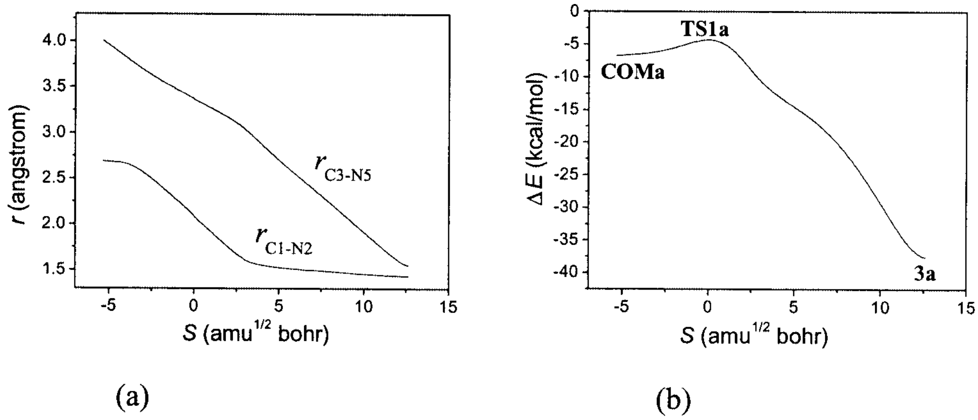

Figure 4. (a) Geometric changes along the IRC; (b) energy change along the IRC (relative to the total energy of reactants and without ZPE correction)

nism can be explained in terms of the Laplacian distributions of electron density in Figure 3, from which it can be seen that only one loose bond (C1−N2) exists in **COMa** and **TS1a**. The geometric changes along IRC in Figure 4 (a), in which the C1−N2 bond length changes dramatically before **TS1a** and that of C3−N5 drops steeply after **TS1a**, confirm the above analysis. In fact, such a transition state is in-between a concerted and a two-step process, which can in general be described as asynchronous.

The solvent effect of the model reaction was also studied at the B3LYP/6-31++G** level with the PCM model and CH_2Cl_2 as a solvent that has been used in experimental investigations. It was found that the structures of all stationary points (see Table S1 of the Supporting Information) were in excellent agreement with those found in the gas phase. The C1−N2 bond in **TS1a** is 0.054Å shorter than that in the gas phase. As reported in our preceding paper,[7a] because the cumulene cation **1** in the solution phase is much more stable than that in the gas phase, the **COMa** complex disappears and the energy of transition state **TS1a** in solution is 5.7 kcal/mol higher than that of the reactants. The obtained results indicate that cycloaddition products **3a** and **4a** in the solution phase are more stable than their gas-phase counterparts, and the energy barrier for rearrangement from **3a** to **4a** is also lowered by 5.5 kcal/mol, which shows that the CH_2Cl_2 solvent favors the [1,2]-H-shift reaction.

Effects of Substituents on the Nitrogen Atom in Isocyanates

This section reports substituent effects with methyl and Cl on the nitrogen atom in isocyanates, such reactions being denoted **1a** + **2b** and **1a** + **2c**, respectively (see Scheme 1). The geometric locations were performed by the B3LYP/6-31++G** method for all the possible stationary points, which are denoted as **COMb**, **TS1b**, **TS2b**, **3b**, and **4b** and as **COMc**, **TS1c**, **TS2c**, **3c**, and **4c**, respectively. The optimized geometric parameters, frequencies, and energies are listed in Tables S4−S9 (Supporting Informations), and the relative energies are shown in Figure 5. The atomic numbering systems of the above stationary points are shown in Scheme 2 (more detailed information is given in Figures S2 and S3 of the Supporting Information).

For the reaction **1a** + **2b**, a complex **COMb** and a transition state **TS1b** were located. The two fragments of the complex were still remote from each other, with the C1−N2 distance being 2.702 Å. In **TS1b**, the C1−N2 and C3−N5 bond lengths are 2.241 and 3.672 Å, respectively, 0.149 and 0.301 Å longer than those in **TS1a** because the bulky substituent (CH_3) on the nitrogen atom has a larger steric effect. From the potential energy surface, it can be seen that the reaction **1a** + **2b** can take place more easily than reaction **1a** + **2a**. If Figure 2 is compared with Figure 5, several points should be pointed out. Firstly, **COMb** has more stabilization energy than **COMa**, due to the electron-donating group on the isocyanate. Secondly, the relative energy of **TS1b** is 2.8 kcal/mol lower than that of **TS1a**, which results in only 1.4 kcal/mol of activation barrier between **COMb** and **3a** via **TS1b** (i.e., 2.2 kcal/mol lower than that in the model reaction). Thirdly, the cycloaddition product **3b** is more stable than **3a** by about 9 kcal/mol. The methyl substituent therefore also favors the rearrangement reaction. The rate-controlling step is still the [1,2]-shift process, which needs to overcome a 20.5 kcal/mol activation barrier, 1.6 kcal/mol lower than that in the model reaction.

When the electron-withdrawing chlorine atom is introduced into the isocyanate, the reaction seems to experience a little more difficulty in taking place than the model reaction. The stabilization energy of **COMc** is 0.2 kcal/mol lower than that of **COMa**, and the activation barrier for the cycloaddition reaction to form **3c** is higher than that in the model reaction (about 1.1 kcal/mol). The reaction can occur easily, however, because the transition state **TS1c** is still below the reactant asymptote. As far as the rearrangement reaction is concerned, the activation barrier and the stabilization energy of rearrangement for the process from **3c** to **4c** are very similar to those for the model reaction.

The above results can easily be interpreted by analysis of frontier molecular orbital interactions. The presence of an electron-releasing substituted group such as methyl on the isocyanate should increase the energy levels of the HOMO

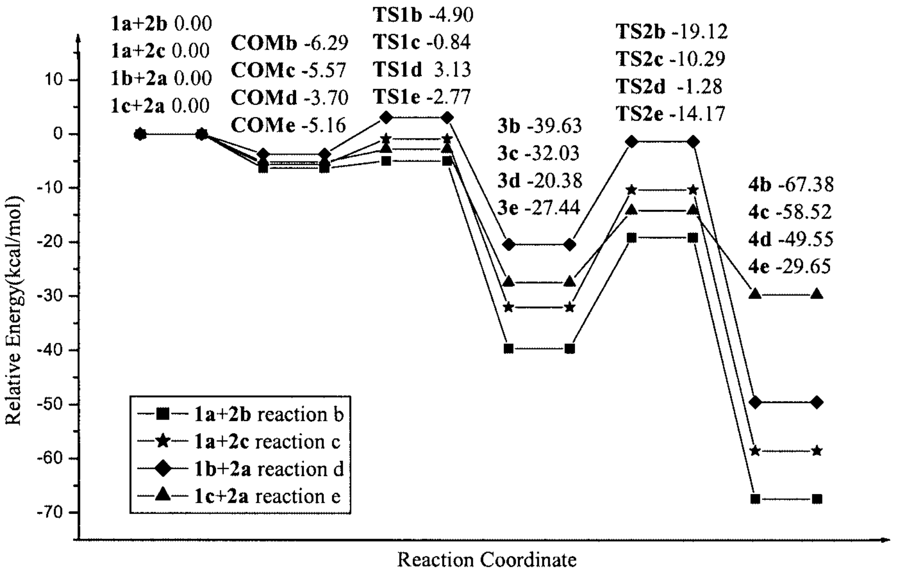

Figure 5. Schematic description of potential energy surfaces for **1a** + **2b**, **1a** + **2c**, **1b** + **2a**, and **1c** + **2a** reactions at the B3LYP/6-31++G** level (with ZPE correction)

and HOMO−1 of the isocyanate, reducing the energy difference between the HOMO or HOMO−1 of **2b** and the LUMO+1 of **1a** and favoring the formation of **3b**. The presence of an electron-withdrawing group in the isocyanate has the reverse effect (i.e., it should disfavor the reaction slightly, which needs to be confirmed by experiments). This trend is similar to our previously reported[7a] substituent effects on olefins in the reactions of **1a** with olefins.

Effects of Substituents on the Carbon Atom of the 1-Aza-2-azoniaallene Cation

The effects of substituents on the carbon atom of the 1-aza-2-azoniaallene cation (see Scheme 1) are reported here. The relative energies of the stationary points for reactions **1b** + **2a** and **1c** + **2a** are given in Figure 5, and the optimized geometric parameters, frequencies, and energies calculated by the B3LYP/6-31++G** method are listed in Tables S10−S15 (Supporting Information), respectively. The atomic numbering systems of the above stationary points are shown in Scheme 2 (more detailed information is given in Figures S4−S5 of the Supporting Information).

The presence of two methyl groups at C1 of the 1-aza-2-azoniaallene cation will affect the C1−N2 bond length through a larger steric effect. The C1−N2 distance in **COMd** becomes 3.187 Å, much longer than those in other complexes. However, the C1−N2 distance in the transition state **TS1d** is 0.023 Å shorter than that in the model reaction, but the C1−N4 bond is 0.047 Å longer than that in the model reaction. Moreover, the main skeleton atoms of **TS1d** are in the same plane, due to favorable steric effects, and the orbital interaction between the LUMO+1 of **1b** and the HOMO−1 of **2a** makes the **TS1d** stable. In products **3d** and **4d**, the C1−N4 distances are 0.021 and 0.016 Å longer, respectively, than those in the model reaction. One of the CH_3 groups may be transferred from C1 to N4 via **TS2d**, to yield the final product **4d**. The charge on the migrating methyl group is 0.29 e (i.e., this methyl group has a partial carbocation character, which is consistent with the reports by Jochims and Kroemer[6i,9e,9f]).

When electron-withdrawing Cl atoms are introduced into cumulene cation **1**, the C=N double bond is obviously lengthened (0.046 Å longer than that in **1a**). Accordingly, the C1−N4 bonds in the following stationary points are all lengthened. The C1−N2 distance in **COMe** is 0.097 Å longer than in **COMa** because the chlorine substituents produce larger steric effects.

As shown in Figure 5, the energy of **COMd** is 2.0 kcal/mol less than that of **COMa**, and **TS1d** is above the reactant asymptote by 4.8 kcal/mol, but 6.8 kcal/mol above **COMd**, which is 3.2 kcal/mol higher than that in the model reaction. Methyl substituents on the carbon atom of the 1-aza-2-azoniaallene cation therefore disfavor the cycloaddition reaction. However, the energy of **TS1e** in the reaction **1c** + **2a** is 1.2 kcal/mol lower than that of **TS1a** in the model reaction, which indicates that the presence of chlorine substituents on the carbon atom of the 1-aza-2-azoniaallene cation should favor the [3+2] cycloaddition reaction slightly. Although the substituents do not change the energy barrier very much, they make **3d**, **3e**, **4d**, and **4e** less stable than their counterparts in the model reaction, especially in the case of **4e**. From the electron densities at the $N-R^1$ bond critical points (see Table S17 in the Supporting Information), it can be seen that the electron densities for N−Cl, N−H, and N−C bonds in **4a**, **4d**, and **4e** are 0.34, 0.24, and 0.21, respectively, which indicates that the N−Cl bond in **4e** is the weakest among the studied systems. As in the case of the activation barriers of the [1,2]-shift reactions, the transition from **3a** to **4a** is the most difficult and that from **3e** to **4e** the easiest. This can be explained in terms of the strength of the bond to be broken. Because the electron density at the C−Cl (ρ_b = 0.20) bond critical point in **3e** is smaller than those of C−H (ρ_b = 0.28) in **3a** and C−C (ρ_b = 0.23) in **3d**, the C−Cl bond strength is less than those of the C−H and C−C bonds, which is favorable for Cl atom migration. In addition, the local energy densities H_b for C−H, C−C, and C−Cl in the intermediates **3a**, **3d**, and **3e** are −1.99, −1.28, and −0.87, respectively, the same trend as the change of ρ_b. In fact, the C−Cl and N−Cl bond strengths are similar, which gives rise to the similar stabilities of **3e** and **4e**, while the energy barrier for a migrating Cl atom is only 13.3 kcal/mol (i.e., they could be transformed into each other easily, which remains to be confirmed by experiments).

Conclusion

From the above discussion, the following conclusions can be drawn:

(1) According to these calculations, all the studied reactions proceed by asynchronous but concerted pathways in the gas phase or in CH_2Cl_2 solution.

(2) Electron-withdrawing chlorine substituents on the 1-aza-2-azoniaallene cation and the electron-releasing methyl substituent on the isocyanate favor the cycloaddition reactions, while electron-releasing methyl substituents on the 1-aza-2-azoniaallene cation and electron-withdrawing chlorine substituents on the isocyanate have the opposite effect.

(3) The activation barriers for cycloaddition reactions are quite low, which is in agreement with the experimentally ascertained fact that these reactions can occur at low temperature.

(4) The presence of Cl substituents on the 1-aza-2-azoniaallene cation dramatically lowers the activation barrier for the [1,2]-shift reactions of cycloaddition products.

Experimental Section

Computational Methods of Calculation: All calculations included in this work were performed with the Gaussian98w program package[10]. The geometries of reactants, products, complexes, intermediates, and transition states were fully optimized. All the geometric parameters of possible stationary points were located at the B3LYP/6-31++G** level and were characterized by the number of imaginary frequencies. For the model reaction (**1a + 2a**), the Polarized Continuum (overlapping spheres) model (PCM)[11] and CH_2Cl_2 solvent (dielectric constant ε = 8.93) were employed to calculate the solvent effects at 298.15 K. In addition, the stationary points for the model reaction were also located and characterized by second-order Mφller-Plesset perturbation theory (MP2) and quadratic configuration interaction calculations, including single and double substitutions (QCISD) methods. For some key reaction paths, Intrinsic Reaction Coordinates (IRCs)[12] were traced to confirm the TS connecting the two corresponding minima. The relative energies of all stationary points were corrected with zero-point vibrational energies. The bonding character and charge distribution for some stationary points were studied on the basis of Bader's AIM theory.[13] The AIM98PC package,[14] a PC version of AIMPAC,[15] was employed for electron density topological analysis with the electron densities obtained by B3LYP/6-31++G** calculation.

Supporting Information: The Z-matrixes, frequencies, energies, and detailed information of atomic numbering systems of all the stationary points are listed in Tables S1−S15 and Figures S1−S5 in the Supporting Information. The charges and the topological properties of electron density distributions of some stationary points are shown in Tables S16−S17 of the Supporting Information.

Acknowledgments

This work was supported by the National Natural Science Foundation of China (20372011 and G2000078100).

[1] [1a] A. Padwa, W. H. Pearson, in *Synthetic Applications of 1,3-Dipolar Cycloaddition Chemistry Toward Heterocycles and Natural Products* (Eds.: K. V. Gothelf, K. A. Jørgensen), John Wiley & Sons, Inc., **2002**, vol. 12, pp. 817−899. [1b] M. Cinquini, F. Cozzi, in *Stereoselective Synthesis* (Eds.: G. Helmchen, R. W. Hoffmann, J. Mulzer, E. Schauman), Georg Thieme, Stuttgart, **1996**, vol. 5, pp. 2953−2987. [1c] A. Padwa, in *Comprehensive Organic Synthesis* (Eds.: B. M. Trost, I. Fleming), Pergamon, Oxford, **1991**, vol. 4, pp. 1069−1109. [1d] P. A. Wade, in *Comprehensive Organic Synthesis* (Eds.: B. M. Trost, I. Fleming), Pergamon, Oxford, **1991**, vol. 4, pp. 1111−1168. [1e] R. Huisgen, in *1,3-Dipolar Cycloaddition Chemistry* (Ed.: A. Padwa), John Wiley & Sons, New York, **1984**, vol. 1, pp. 1−176.

[2] For example: [2a] G. Y. Li, J. Chen, W. Y. Yu, W. Hong, C. M. Che, *Org. Lett.* **2003**, *5*, 2153−2156. [2b] S. Caddick, H. D. Bush, *Org. Lett.* **2003**, *5*, 2489−2492. [2c] A. A. Raj, R. Raghunathan, *Tetrahedron* **2003**, *59*, 2907−2911. [2d] S. Collon, C. Kouklovsky, Y. Langlois, *Eur. J. Org. Chem.* **2002**, 3566−3572. [2e] J. M. Longmire, B. Wang, X. Zhang, *J. Am. Chem. Soc.* **2002**, *124*, 13400−13401.

[3] For example: [3a] E. Rajaian, M. Monajjemi, M. R. Gholami, *J. Chem. Res. (S)* **2002**, 279−281. [3b] K. N. Houk, J. Gonzalez, Y. Li, *Acc. Chem. Res.* **1995**, *28*, 81−90. [3c] R. Huisgen, *J. Org. Chem.* **1976**, *41*, 403−419. [3d] A. Rastelli, R. Gandolfi, M. Sarzi-Amade, B. Carboni, *J. Org. Chem.* **2001**, *66*, 2449−2458. [3e] Y. Hu, K. N. Houk, *Tetrahedron* **2000**, *56*, 8239−8243.

[4] For example: [4a] W. Wirschun, J. C. Jochims, *Synthesis* **1997**, 233−245. [4b] W. Wirschun, M. Winkler, K. Lutz, J. C. Jochims, *J. Chem. Soc., Perkin Trans. 1* **1998**, 1755−1762. [4c] S. Parsons, J. Passmore, M. J. Schriver, X. Sun, *Inorg. Chem.* **1991**, *30*, 3342−3348. [4d] N. Burford, J. P. Johnson, J. Passmore, M. J. Schriver, P. S. White, *J. Chem. Soc., Chem. Commun.* **1986**, 966−968.

[5] [5a] M. Okimoto, T. Chiba, *J. Org. Chem.* **1990**, *55*, 1070−1076. [5b] R. N. Butler, *Chem. Rev.* **1984**, *84*, 249−276. [5c] O. Hammerich, V. D. Parker, *J. Chem. Soc., Perkin Trans. I* **1972**, 1718−1720. [5d] E. Gunic, I. Tabakovic, *J. Org. Chem.* **1988**, *53*, 5081−5087. [5e] J. Warkentin, *Synthesis* **1970**, 279−286. [5f] E.-C. Lin, M. R. Van De Mark, *J. Chem. Soc., Chem. Commun.* **1982**, 1176−1178. [5g] S. Crljenak, I. Tabakovic, D. Jeremic, I. Gaon, *Acta Chem. Scand., Ser. B* **1983**, *37*, 527−535.

[6] For example: [6a] Q. Wang, J. C. Jochims, S. Kohlbrandt, L. Dahlenburg, M. Al-Taib, A. Hamed, A. E. Ismail, *Synthesis* **1992**, 710−718. [6b] N. A. Hassan, T. K. Mohamed, O. M. Abdel Hafez, M. Lutz, C. C. Karl, W. Wirschun, Y. A. Al-Soud, J. C. Jochims, *J. Prakt. Chem.* **1998**, *340*, 151−159. [6c] Y. A. Al-Soud, W. Wirschun, N. A. Hassan, G.-M. Maier, J. C. Jochims, *Synthesis* **1998**, 721−728. [6d] Q. Wang, A. Amer, S. Mohr, E. Ertel, J. C. Jochims, *Tetrahedron* **1993**, *49*, 9973−9986. [6e] Y. Guo, Q. Wang, J. C. Jochims, *Synthesis* **1996**, 274−280. [6f] W. G. Wirschun, Y. A. Al-Soud, K. A. Nusser, O. Orama, G. M.

Maier, J. C. Jochims, *J. Chem. Soc., Perkin Trans. 1* **2000**, 4356−4365. [6g] Q. Wang, A. Amer, C. Troll, H. Fischer, J. C. Jochims, *Chem. Ber.* **1993**, *126*, 2519−2524. [6h] Q. Wang, M. Al-Taib, J. C. Jochims, *Chem. Ber.* **1994**, *127*, 541−547. [6i] Q. Wang, S. Mohr, J. C. Jochims, *Chem. Ber.* **1994**, *127*, 947−953. [6j] N. Al-Masoudi, N. A. Hassan, Y. A. Al-Soud, P. Schmidt, A. E.-D. M. Gaafar, M. Weng, S. Marino, A. Schoch, A. Amer, J. C. Jochims, *J. Chem. Soc., Perkin Trans. 1* **1998**, 947−954. [6k] Y. A. Al-Soud, P. B. Shrestha-Dawadi, M. Winkler, W. Wirschun, J. C. Jochims, *J. Chem. Soc., Perkin Trans. 1* **1998**, 3759−3766. [6l] A. B. A. El-Gazzar, K. Scholten, Y. Guo, K. Weißenbach, M. G. Hitzler, G. Roth, H. Fischer, J. C. Jochims, *J. Chem. Soc., Perkin Trans. 1* **1999**, 1999−2010. [6m] N. A. Al-Masoudi, Y. A. Al-Soud, A. Geyer, *Tetrahedron* **1999**, *55*, 751−758. [6n] X. Liu, Y. Liu, Q. Wang, *Synth. Commun.* **2000**, *30*, 119−130. [6o] A. B. A. El-Gazzar, M. I. Hegab, N. A. Hassan, *Sulfur Lett.* **2002**, *25*, 45−62.

[7] [7a] M. J. Wei, D. C. Fang, R. Z. Liu, *J. Org. Chem.* **2002**, *67*, 7432−7438. [7b] W. J. Ding, D. C. Fang, *J. Org. Chem.* **2001**, *66*, 6673−6678. [7c] S. Y. Yang, C. K. Sun, D. C. Fang, *J. Org. Chem.* **2002**, *67*, 3841−3846. [7d] S. Y. Yang, C. K. Sun, D. C. Fang, *Eur. J. Org. Chem.* **2003**, 1942−1947. [7e] Y. Q. Ding, D. C. Fang, *J. Org. Chem.* **2003**, *68*, 4382−4387.

[8] [8a] H. Gstach, P. Seil, J. G. Schantl, A. Gieren, T. Hübner, J. Wu, *Angew. Chem. Int. Ed. Engl.* **1986**, *25*, 1132−1134. [8b] J. G. Schantl, N. Lanznaster, H. Gstach, *Heterocycles* **1990**, *31*, 833−840. [8c] J. G. Schantl, N. Lanznaster, H. Gstach, *Heterocycles* **1990**, *31*, 825−832.

[9] [9a] H. Gstach, P. Seil, *Synthesis* **1990**, 803−808. [9b] H. Gstach, P. Seil, *Synthesis* **1990**, 808−815. [9c] H. Gstach, P. Seil, *Synthesis* **1990**, 1048−1053. [9d] H. Schildknecht, G. Hatzmann, *Angew. Chem. Int. Ed. Engl.* **1986**, *8*, 456. [9e] R. T. Kroemer, H. Gstach, K. R. Liedl, B. M. Rode, *J. Am. Chem. Soc.* **1994**, *116*, 6277−6283. [9f] R. T. Kroemer, H. Gstach, K. R. Liedl, B. M. Rode, *J. Chem. Soc., Perkin Trans. 2* **1994**, 2129−2135.

[10] M. J. Frisch, G. W. Trucks, H. B. Schlegel, G. E. Scuseria, M. A. Robb, J. R. Cheeseman, V. G. Zakrzewski, J. A. Montgomery, Jr., R. E. Stratmann, J. C. Burant, S. Dapprich, J. M. Millam, A. D. Daniels, K. N. Kudin, M. C. Strain, O. Farkas, J. Tomasi, V. Barone, M. Cossi, R. Cammi, B. Mennucci, C. Pomelli, C. Adamo, S. Clifford, J. Ochterski, G. A. Petersson, P. Y. Ayala, Q. Cui, K. Morokuma, D. K. Malick, A. D. Rabuck, K. Raghavachari, J. B. Foresman, J. Cioslowski, J. V. Ortiz, A. G. Baboul, B. B. Stefanov, G. Liu, A. Liashenko, P. Piskorz, I. Komaromi, R. Gomperts, R. L. Martin, D. J. Fox, T. Keith, M. A. Al-Laham, C. Y. Peng, A. Nanayakkara, M. Challacombe, P. M. W. Gill, B. Johnson, W. Chen, M. W. Wong, J. L. Andres, C. Gonzalez, M. Head-Gordon, E. S. Replogle, J. A. Pople, *GAUSSIAN 98*, Gaussian, Inc., Pittsburgh PA, **1998**.

[11] [11a] S. Miertus, E. Scrocco, J. Tomasi, *Chem. Phys.* **1981**, *55*, 117−129. [11b] S. Miertus, J. Tomasi, *Chem. Phys.* **1982**, *65*, 239−245. [11c] M. Cossi, V. Barone, R. Cammi, J. Tomasi, *Chem. Phys. Lett.* **1996**, *255*, 327−335. [11d] M. T. Cances, V. Mennucci, J. Tomasi, *J. Chem. Phys.* **1997**, *107*, 3032−3041. [11e] V. Barone, M. Cossi, B. Mennucci, J. Tomasi, *J. Chem. Phys.* **1997**, *107*, 3210−3221. [11f] M. Cossi, V. Barone, B. Mennucci, J. Tomasi, *Chem. Phys. Lett.* **1998**, *286*, 253−260. [11g] V. Barone, M. Cossi, J. Tomasi, *J. Comp. Chem.* **1998**, *19*, 404−417. [11h] V. Barone, M. Cossi, *J. Phys. Chem. A* **1998**, *102*, 1995−2001. [11i] B. Mennucci, J. Tomasi, *J. Chem. Phys.* **1997**, *106*, 5151−5158.

[12] [12a] C. Gonzalez, H. B. Schlegel, *J. Chem. Phys.* **1989**, *90*, 2154−2161. [12b] Gonzalez, C. H. B. Schlegel, *J. Phys. Chem.* **1990**, *94*, 5523−5527.

[13] [13a] R. F. W. Bader, *Chem. Rev.* **1991**, *91*, 893−928. [13b] R. F. W. Bader, *Atoms in molecules, a Quantum Theory*, Clarendon Press, Oxford, **1990**.

[14] D. C. Fang, T. H. Tang, *AIM98PC, the PC version of AIMPAC*, Beijing Normal University, Beijing, China.

[15] Available from Professor R. F. W. Bader's Laboratory, McMaster University, Hamilton, Ontario, Canada, L8S 4M1.

Received May 15, 2004